ACCESS
Arctic Climate Change
Economy and Society

Project no. 265863

ACCESS

Arctic Climate Change, Economy and Society

Instrument: Collaborative Project
Thematic Priority: Ocean.2010-1 "Quantification of climate change impacts on economic sectors in the Arctic"

D1.72 – Model output from CTM studies of the impact on composition from changes in emissions

Due date of deliverable: **31/08/2013**

Actual submission date: **04/02/2014**

Start date of project: **March 1st, 2011** Duration: **48 months**

Organisation name of lead contractor for this deliverable: **CICERO**

Project co-funded by the European Commission within the Seventh Framework Programme (2007-2013)		
Dissemination Level		
PU	Public	X
PP	Restricted to other programme participants (including the Commission Services)	
RE	Restricted to a group specified by the consortium (including the Commission Services)	
CO	Confidential, only for members of the consortium (including the Commission Services)	

Contents

1. Impact from local Arctic sources

In WP1 Deliverables D1.71 and D1.72 in ACCESS studies were made to quantify impacts on climate and air pollution levels of local Arctic emission sources both for the current and future. These are performed in synergy and addition to chemistry-climate work in WP2 and WP4 which is focusing on smaller scales using campaign data. The OsloCTM2 model and a Radiative Forcing (RF) model were used to study the evolution of chemical constituents causing impacts in the Arctic. The RF results and impacts on climate will be presented in Deliverable D1.71. This report focuses on the composition changes of air pollutants calculated by the CTM.

In the closely related project ArcAct, Ødemark et al. (2012) calculated current impacts from petroleum activity and shipping in the Arctic.

Specifically for ACCESS a new paper (Dalsøren et al. 2013) calculates impacts of future global and Arctic shipping with a particular focus on different scenarios for soot emissions. Corbett et al. (2010) provides gridded inventories for current (2004) and future (2030, 2050) ship emissions of greenhouse gases and gas and particulate pollutants in the Arctic. That study presents several options for emission totals and diversion routes through the Arctic in 2030. In this study we compare their highest and lowest 2030 estimates to get an impression of the range of possible future effects due to emissions of NOx, SOx, CO, NMVOCs, BC and OC (Table 1). The two datasets for ship emissions are used to characterize the potential impact from shipping and the degree to which shipping controls may mitigate impacts: A high (HIGH) scenario and a low scenario with Maximum Feasible Reduction (MFR) of black carbon in the Arctic. In the high growth scenario (HIGH) there is a large increase in ship traffic within the Arctic. In addition 2 % of the yearly global traffic diverts to Arctic through-routes during late summer. Global shipping growth outside the Arctic is + 3.3% per year. In the Maximum Feasible Reduction (MFR) scenario a business as usual scenario is followed but maximum feasible reduction is applied on Arctic BC emissions (also affecting OC). In this scenario, 1 % of the global traffic (the business as usual scenario from Corbett et al. 2010a) diverts to Arctic through-routes. Global shipping growth outside the Arctic is + 2.1 % per year. In MFR, BC emissions in the Arctic are reduced with 70 % representing a combination technology performance and/or reasonable advances in single-technology performance. Counteracting the traffic growth in both scenarios is a phase in of existing regulations,

resulting in reduced emission factors for some components. The emission scenarios are described in detail in Corbett et al. (2010).

	NO_x	SO_2	BC	OC
2004	**196**	**136**	**0.88**	**2.70**
2030 HIGH	**739**	**130**	**4.50**	**5.10**
Arctic fleet	329	58	2.00	2.30
Diversion fleet	410	72	2.50	2.80
2030 MFR	**384**	**68**	**0.76**	**0.84**
Arctic fleet	244	43	0.46	0.51
Diversion fleet	140	25	0.30	0.33

Table 1: Ship emissions north of 60° N in 2004 and 2030 (Kton/year) from Corbett et al. (2010). There is seasonal variation in the emissions from the Arctic fleet. The diversion fleet operates in the period August-October.

To calculate the impacts on pollution and chemical composition the OsloCTM2 model was used. Simulations were performed in T42 resolution (2.8°x 2.8°) with 60 vertical layers using meteorological data for 2006. The tropospheric distributions of 137 chemical species are calculated, amongst them hydrogen, oxygen, nitrogen, and carbon containing gases and also sulfate, nitrate, primary organic, secondary organic, black carbon (BC), and sea salt aerosols.

For all species tropospheric concentration changes vary strongly in magnitude and distribution with season, in particular in the Arctic where photochemistry is most active during a few summer months.

In both future scenarios the surface NO_2 changes are found close to or within the shipping lanes (Figure 1). Increases from 2004 to 2030 are typically in the range 10 % to above 60 % in coastal regions of the Northern Hemisphere, Arctic shipping regions, and main oceans shipping lanes in both hemispheres. In late summer, when operation takes place along the diversion routes, increases are above 200 % in pristine regions of the Arctic. The largest NO_2 changes are found for the HIGH scenario. For surface ozone the HIGH scenario shows substantial increases of 2 to above 5 ppv (4 to above 10 %) in coastal and oceanic regions of the Northern Hemisphere (Figure 2). In pristine regions of the tropical and Arctic Oceans the increases are above 10 %. The changes in the MFR scenario are moderate and a few ppbv/percent over the oceans and coastal areas.

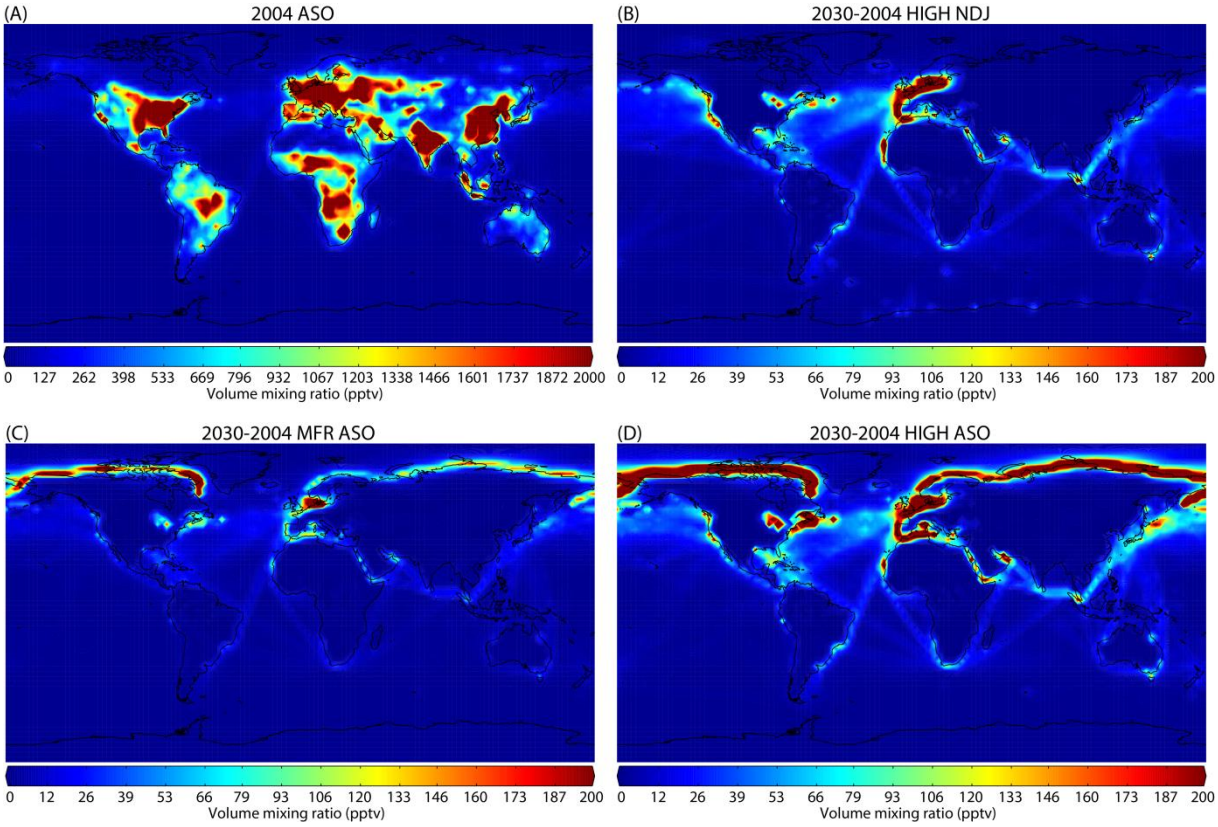

Figure 1: NO_2 in the lowest model layer close to the surface (pptv). **(A)** Average 2004 for the months August-Sept-Oct (ASO). **(B)** Average change 2004-2030 for HIGH scenario for the months November-Dec-Jan (NDJ). **(C)** Same as (B), MFR scenario, months ASO. **(D)** Same as (B), HIGH scenario, months ASO.

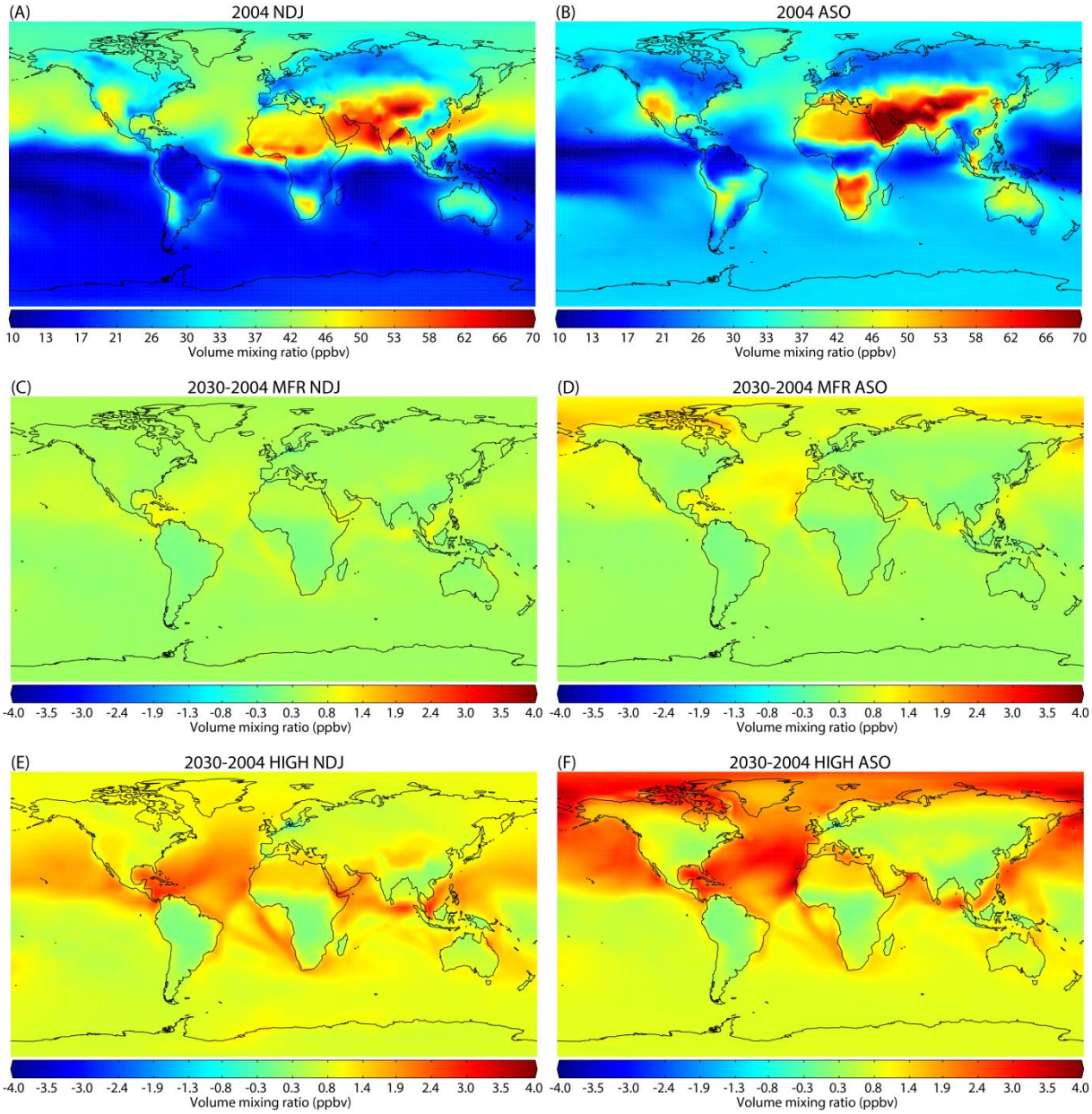

Figure 2: O_3 in the lowest model layer close to the surface (ppbv). Averages 2004 for the months November-Dec-Jan (NDJ) **(A)** and August-Sept-Oct (ASO) **(B)**. Average change 2004-2030 MFR scenario for the months NDJ **(C)** and ASO **(D)**. Average Change 2004-2030 HIGH scenario for the months NDJ **(E)** and ASO **(F)**.

Due to regulations, reductions in future sulfate levels are found at mid-latitudes (Figure 3). On the west coast of the continents reduction around 50 pptv or 10-15 % is important and could reduce health impact from particle pollution and acid precipitation. Increases (up to 50 %) are only found in regions near the diversion routes in the Arctic in the months of operation.

OC emissions correlate with sulfur emissions and surface OC shows relative reductions of about 5 % both at mid and polar latitudes. The diversion routes in the late summer season are an exception to this, with increases of 10-30 % in the HIGH scenario.

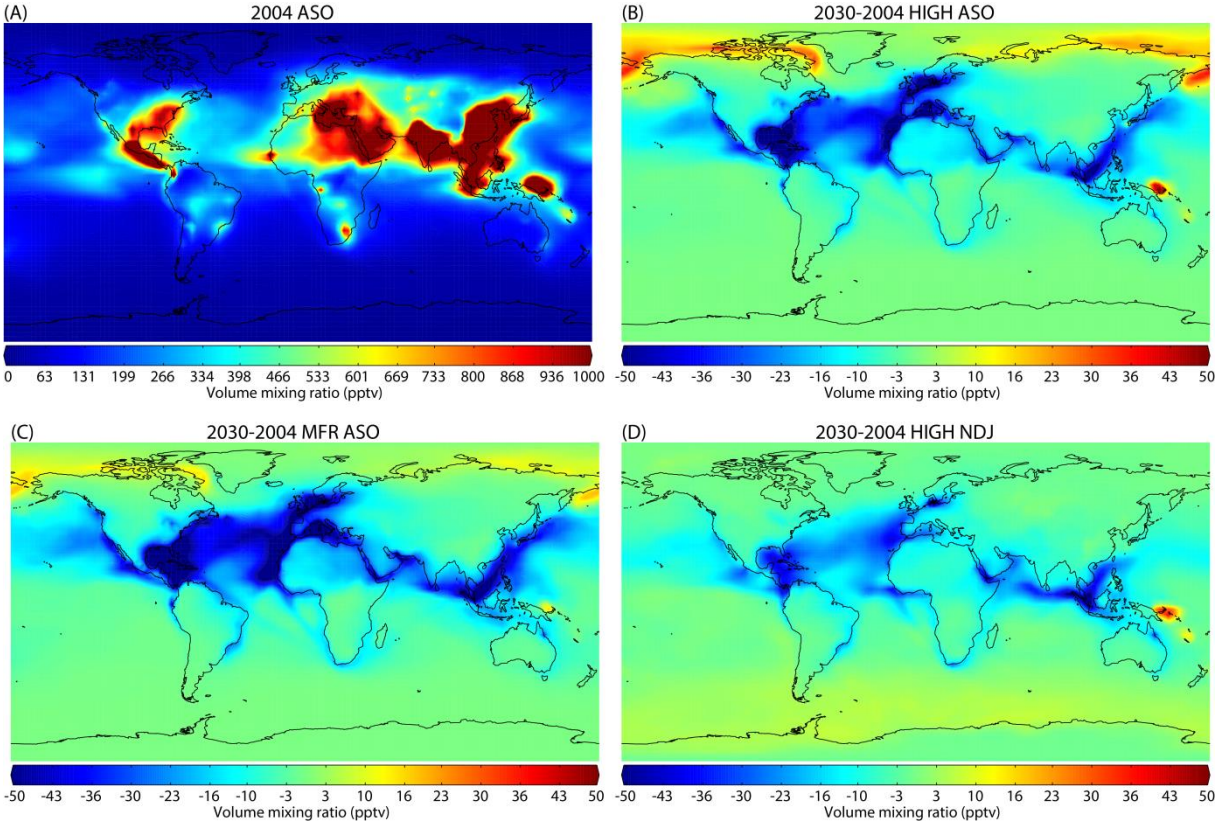

Figure 3: Sulfate in the lowest model layer close to the surface (pptv). **(A)** Average 2004 for the months August-Sept-Oct (ASO). **(B)** Average change 2004-2030 HIGH scenario for the months ASO. **(C)** Same as (B), MFR scenario **(D)** Same as (B), HIGH scenario, months November-December-January (NDJ).

The largest absolute surface BC increases are found in the North Sea and other regions with much traffic (Figure 4). In late summer the MFR scenario has a decrease of about 10 % in Arctic regions with internal traffic, and a similar or larger increase in the regions with diversion traffic. For the HIGH scenario the BC levels increase more than 50 % in much of the Arctic in late summer.

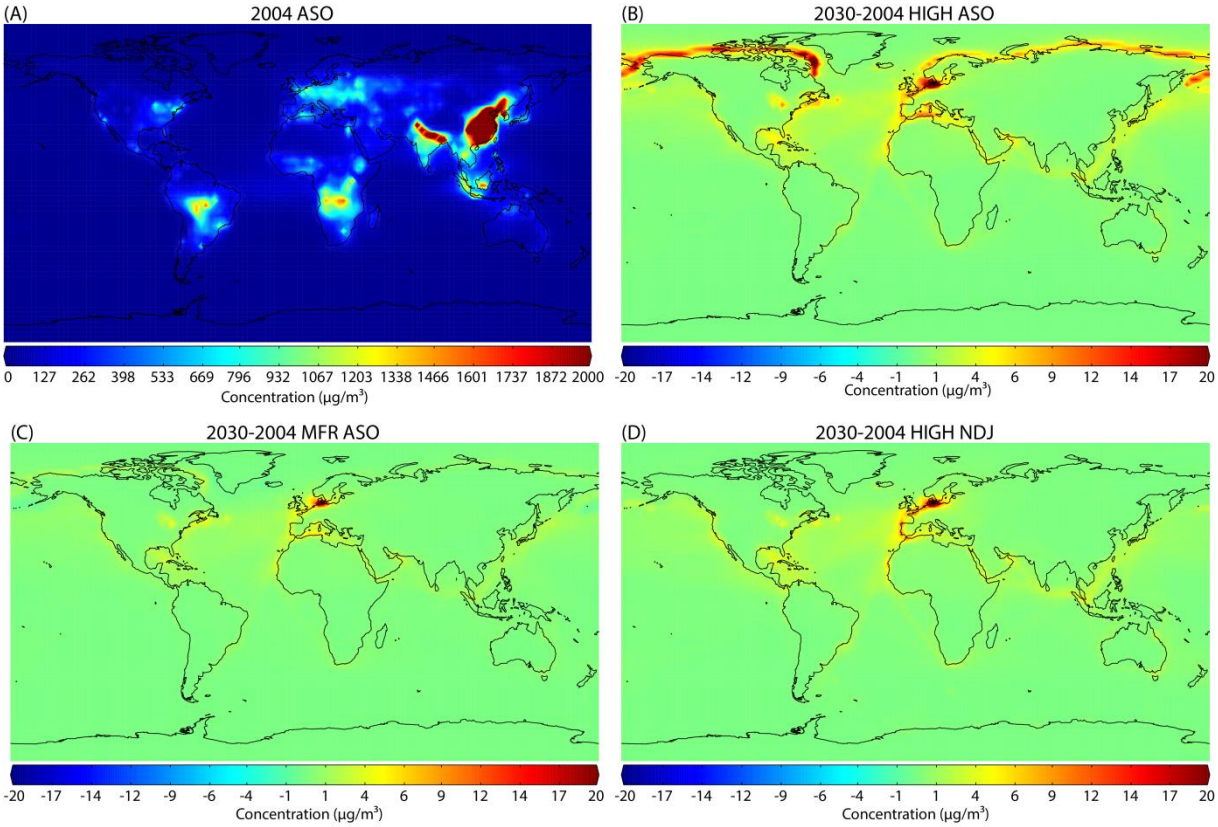

Figure 4: Same as Figure 3 for BC (µg/m^3).

To summarize, both scenarios result in moderate to substantial increases in concentrations of pollutants both globally and in the Arctic. Exceptions are black carbon in the MFR scenario, and sulfur species and organic carbon in both scenarios due to the future phase-in of current regulation that reduces fuel sulfur content. So phasing in of existing IMO regulations on sulfate are efficient in reducing particle pollution both globally and in the Arctic. In the season with potential transit traffic through the Arctic in 2030 we find increased concentrations of all pollutants in large parts of the Arctic.

2. Impact from sources outside the Arctic

In addition to local, emerging pollution sources including ships work has focused on pollution transport into the Arctic from mid-latitudes. A full analysis of inter-annual variation of pollutant transport to the Arctic will be made in D1.52. But already a paper has been published on the long-range transport of pollution plumes from anthropogenic and fire emissions to the Arctic in the summer 2008 (Thomas et al., 2013). In summer 2008 aircraft campaigns focused on measuring pollution during transport to the Arctic from North American anthropogenic and biomass burning sources as part of the International Polar Year POLARCAT campaigns. We have used POLARCAT (Polar Study using Aircraft, Remote Sensing, Surface Measurements and Models, of Climate, Chemistry, Aerosols, and Transport) data combined with a high resolution chemical transport model (WRF-Chem) to understand photochemical ozone production in plumes originating from Canadian biomass burning and North American anthropogenic pollution during summer 2008 (model domain shown in Figure 5). We focus on a period when multiple aircraft were flying in different regions (N. America and Greenland) with the specific aim of studying ozone pollution, which is formed photochemically in the atmosphere either before or during long-range transport. Transport of pollution contributes to both background and episodic ozone levels in the Arctic. Model results were evaluated using POLARCAT aircraft data collected over boreal fire source regions in Canada (ARCTAS-B) and several days downwind over Greenland (POLARCAT-France and POLARCAT-GRACE) during the study period (flights are shown in Figure 5).

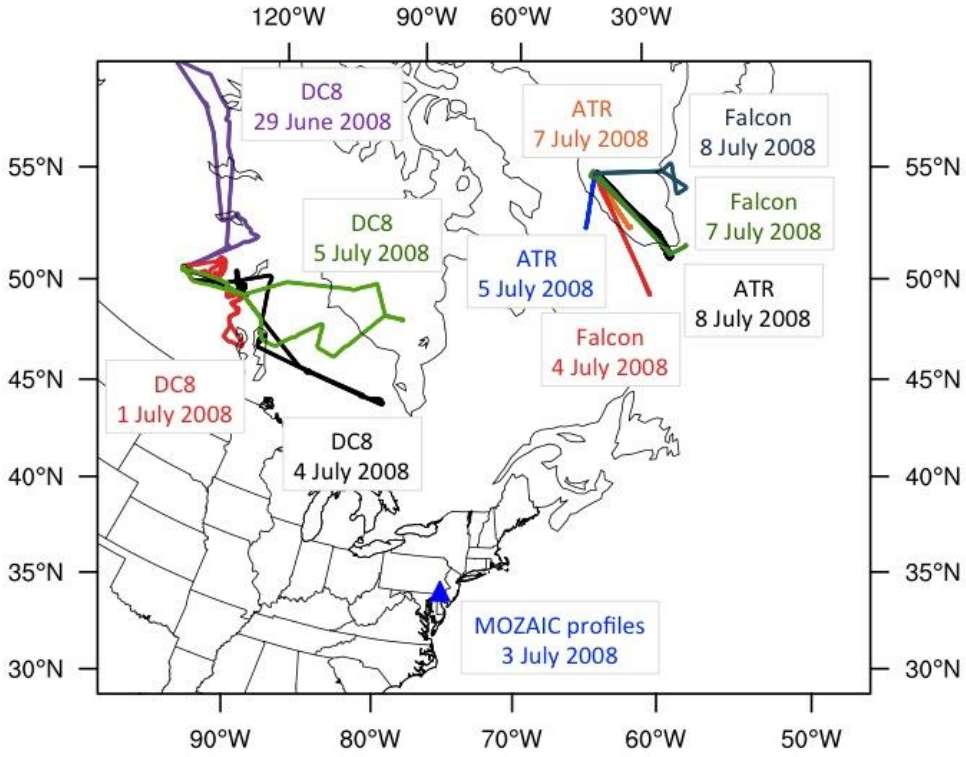

Figure 5. Map of the WRF-Chem domain and the flights conducted as part of POLARCAT used to evaluate the model. The NASA DC8 flights are shown in purple (29 June), red (1 July), black (4 July) and green (5 July). The ATR-42 flights are shown in blue (5 July), orange (7 July), and black (8 July). The Falcon-20 flights are shown in red (4 July), green (7 July), and dark blue (8 July). The location of the two MOZAIC (Measurement of Ozone and Water Vapor by Airbus In-Service Aircraft) profiles of the troposphere during flights in and out of Philadelphia, Pennsylvania on 3 July is shown by the blue triangle.

Regional chemical transport model (CTM) simulations were performed using the Weather Research and Forecasting model including gas and aerosol chemistry (WRF-Chem Version 3.3) (Grell et al., 2005, Fast et al., 2006). The model was run from 28 June 2008 to 9 July 2008 using a polar-stereographic grid (35×35 km resolution) over a domain encompassing boreal fires and anthropogenic emission regions and downwind over Greenland. The specifics of the model setup are detailed in Thomas et al., 2013. Model runs used the anthropogenic emission inventory developed for NASA ARCTAS (The Arctic Research of the Composition of the Troposphere from Aircraft and Satellites) by D. Streets and Q. Zhang (http://www.cgrer.uiowa.edu/arctas/emission.html). Fire emissions were included using the Fire INventory from NCAR (FINNv1) (Wiedinmyer et al., 2006, 2011), with a diurnal profile as described in Pfister et al. (2011). Fire emissions were distributed vertically using the online plume rise module of Freitas et al., 2007, which was recently shown to perform well for the fires observed during ARCTAS (Sessions et al., 2011). Biogenic emissions were from Model of Emissions of Gases and Aerosols from Nature (MEGAN) (Guenther et al., 2006). Three

WRF-Chem model runs were performed: a base run with all emissions included; a run without fire emissions (noFire run); and a run without anthropogenic emissions (noAnthro run). In the latter 2 cases, the respective emissions (fire or anthropogenic) were switched off for the duration of the run inside the regional model domain.

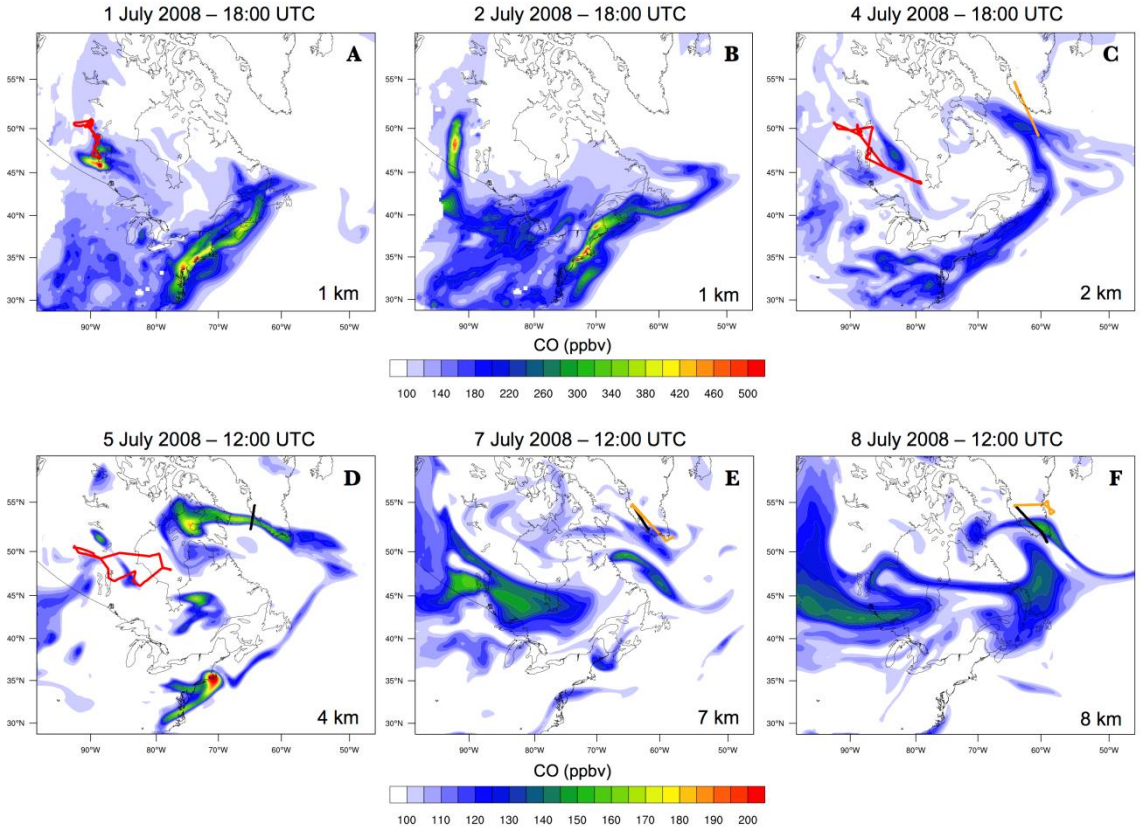

Figure 6. Maps of pollution plumes, as indicated by model predicted CO concentrations above 100 ppbv, between 29 June and 8 July. DC8 flight tracks are shown in red, ATR-42 flight tracks are shown in black, and Falcon-20 flight tracks are shown in orange.

During the focus period of the pollution plumes were transported east and north towards the Arctic. Figure 6 shows examples of modeled plumes at altitudes of 1 and 2 km (indicated by CO mixing ratios >100 ppbv) over the fire and anthropogenic source regions in early July (Figure 6, panels A-C) that were transported towards the Arctic and sampled later downwind by the French and German aircraft at 4, 7, and 8 km (Figure 6, Panels D-F). Very concentrated pollution plumes (CO concentrations greater than 200 ppbv) are diluted in the atmosphere during transport, resulting in less concentrated, more dispersed plumes after transport.

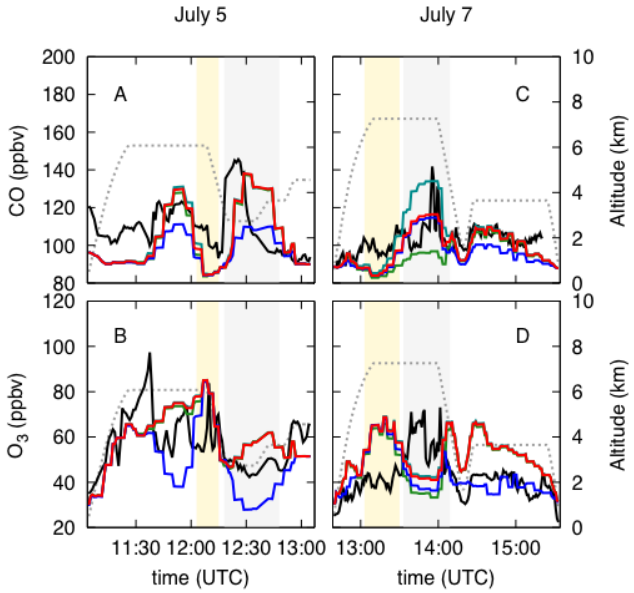

Figure 7. Comparison of WRF-Chem results with measurements made onboard the ATR-42 aircraft on 5 and 7 July. Measurements are in black, the model base run is in red, the noFire run is in green, the noAnthro run is in blue, and the FireCOSens run is in teal. The dashed line represents the aircraft altitude. The anthropogenic plumes investigated in more detail are highlighted using the gray background. High ozone airmasses during the flight on 7 July are shown in yellow.

In order to evaluate the representation of aged biomass burning and anthropogenic plumes measured over southern Greenland we use data collected onboard the French and German aircraft, which targeted aged pollution during POLARCAT. For the ATR-42, CO (Figure 7A) and ozone (Figure 7B) the results from the base case agree well with the measurements in the mid-troposphere. In the upper troposphere, modeled CO is too low, for example at 8 km, 150 ppbv was measured compared to 120 ppbv in the model. The FireCOSens run, with additional CO emissions, is in better agreement with CO measurements in the upper troposphere. This shows that the amount of CO emissions in North America impacts CO levels in the free troposphere downwind because plumes are strongly uplifted during transport. This shows that the low bias in CO is primarily due to Canadian fire emissions in the base run. Imperfect representation of the location of plumes in the model may be another cause of the low bias in modeled fire plumes downwind. Figure 6F clearly shows this airmass was in the region of the aircraft, but the modeled peak CO concentrations (~160 ppbv at 8 km) are east of the flight track. For the Falcon-20 flights, CO between 6-9 km is too low in the base model run (Figure 7C), for example, at 8 km, 130 ppbv was measured compared to 90 ppbv peak in the model. Again, the FireCOSens run is in better agreement with the measured CO levels, but still contains a low bias (~20 ppbv) in the mid and upper

troposphere. As already discussed for the ATR-42 comparisons, plume location is also an important factor in the low bias. For example, on 8 July, the modeled fire plume is south of the Falcon-20 flight track (Figure 6F), suggesting that uncertainties in modeling the transport between North America and Greenland may also contribute.

We use the Lagrangian Particle Dispersion model FLEXPART (Stohl et al., 2005) to investigate the origin of the plumes sampled by the ATR-42 on 5 and 7 July (highlighted in gray in Figure 7A and 7C. Emissions sensitivities were calculated backwards from the time and altitude of the plumes. For the plume measured on 5 July the emissions sensitivities (Figure 8A) confirm the plume is anthropogenic in origin, with contributions from the northeastern United States 3-5 days before the plume was measured over southern Greenland. The FLEXPART emission sensitivities for the plume on 7 July show that it originated from the BB region over Canada (Figure 8B) 5-7 days before the flight, indicating longer transport time than for anthropogenic plumes.

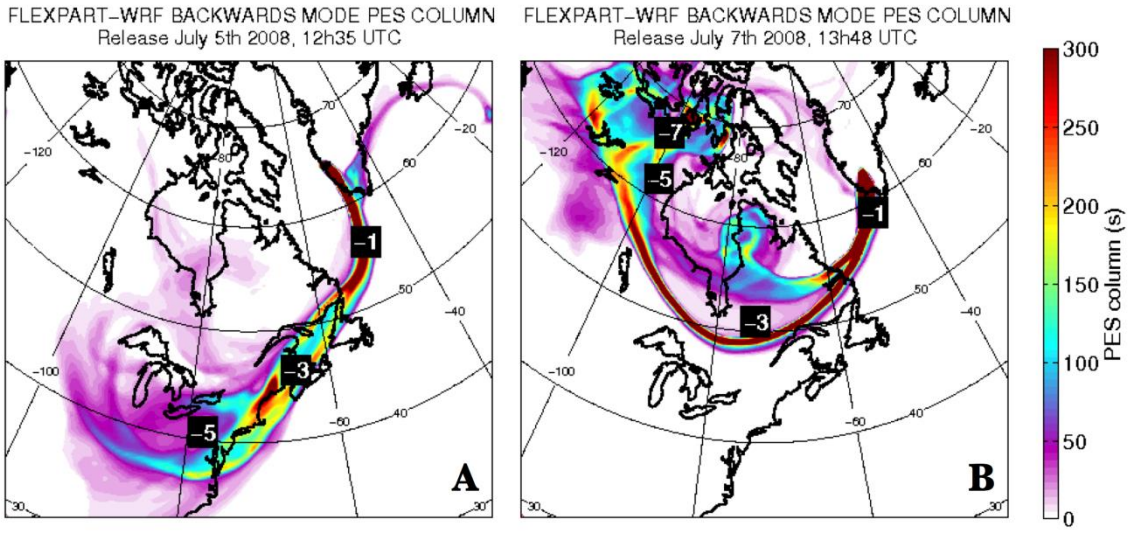

Figure 8. FLEXPART-WRF potential emissions sensitivities (PES) for the second plume sampled by the ATR-42 aircraft on 5 July 2008 at 12:30 UTC (A) and the first plume sampled on 7 July 2008 at 13:45 UTC (B), the location of the average emission sensitivity for each day prior to the release time are also indicated in white. The emissions sensitivities show clearly that the plumes have different origins; the plume sampled on 5 July is anthropogenic in origin, while the first plume on 7 July originates from the region where boreal forest fires were burning in June-July 2008.

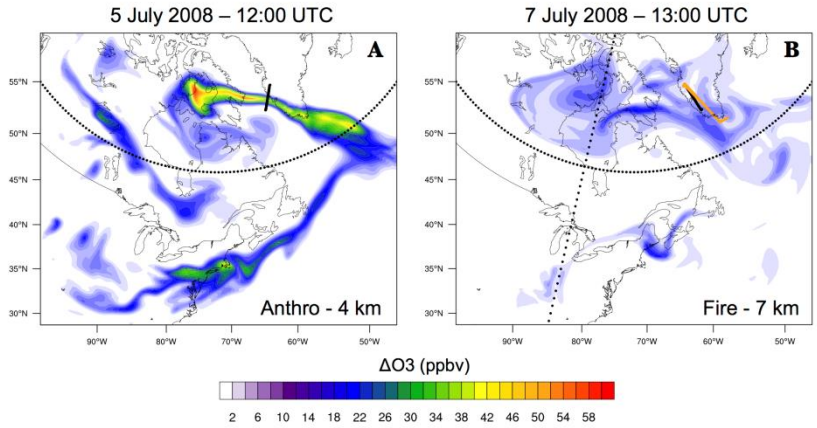

Figure 9. Maps of enhancements in ozone in anthropogenic and fire plumes (ΔO3) demonstrating the spatial extent of plumes sampled by the ATR-72 and Falcon-20 on 5 and 7 July 2008. The ATR-42 aircraft flight tracks are in black and the Falcon-20 flight track is in orange. For anthropogenic plumes, the latitude 55 °N that is used in the following figures is indicated by the dotted black line. For fire plumes, the latitude 55 °N longitude 85 °W are both indicated by dotted black lines.

The spatial extent of the increase in ozone (ΔO3) due to anthropogenic and fire plumes (where $\Delta O3_{Anthro} = O3_{base}-O3_{noAnthro}$ and $\Delta O3_{Fire} = O3_{base}-O3_{noFire)}$ encountered by the ATR-42 on 5 July and 7 July are shown in Figure 9. On 5 July (Figure 9A), the ATR-42 transected a large anthropogenic pollution plume with ozone enhancements up to 60 ppbv. During the flight on 7 July (Figure 9B), the model predicts ozone enhancements of up to 20 ppbv in fire plumes at 7 km.

To summarize, both anthropogenic and fire plumes result in increased ozone concentrations in the Arctic. During the focus period, we calculated the average ozone increase due to emissions after plume aging (where aged plumes are defined as: latitude>55 °N for anthropogenic emissions, latitude>55 °N and longitude<85 °W for fire emissions). During the study period (29 June to 9 July 2008), anthropogenic pollution from North America increases ozone by up to 6.5 ppbv in the lower to mid-troposphere and boreal fire pollution increases ozone by up to 3 ppbv in the mid/upper troposphere. Our study is based on a relatively short period of time, when there was active transport of both fire and anthropogenic plumes from North America to the east and north into the Arctic. However, our findings suggest a significant contribution to tropospheric ozone at higher latitudes from both anthropogenic and fire pollution transported toward the Arctic. These enhancements represent an increase in ozone of up to 18% from anthropogenic emissions (mid troposphere) and an increase of up to 5.2% from biomass burning (upper troposphere). These increases cannot be disregarded considering the relatively low background ozone concentrations in the Arctic.

References

Corbett, J., Lack, D., Winebrake, J., Harder, S., Silberman, J., and Gold, M.: Arctic shipping emissions inventories and future scenarios, Atmospheric Chemistry and Physics, 10, 9689-9704, DOI 10.5194/acp-10-9689-2010, 2010.

Dalsøren, S. B., Samset, B. H., Myhre, G., Corbett, J. J., Minjares, R., Lack, D., and Fuglestvedt, J. S.: Environmental impacts of shipping in 2030 with a particular focus on the Arctic region, Atmos. Chem. Phys., 13, 1941-1955, doi:10.5194/acp-13-1941-2013, 2013.

Fast, J. D., Gustafson W. I. Jr., W., Easter, R., Zaveri, R. A., Barnard, J. C., Chapman, E. G., Grell, G., and Peckham, S.: Evolution of ozone, particulates, and aerosol direct radiative forcing in the vicinity of Houston using a fully coupled meteorology-chemistry-aerosol model, J. Geophys. Res., 111, D21305, doi:10.1029/2005JD006721, 2006.

Freitas, S. R., Longo, K. M., Chatfield, R., Latham, D., Silva Dias, M. A. F., Andreae, M. O., Prins, E., Santos, J. C., Gielow, R., and Carvalho, J. A. Jr.: Including the sub-grid scale plume rise of vegetation fires in low resolution atmospheric transport models, Atmos. Chem. Phys., 7, 3385-3398, doi:10.5194/acp-7-3385-2007, 2007.

Grell, G. A., Peckham, S. E., Schmitz, R., McKeen, S. A., Frost, G., Skamarock, W. C., and Eder, B.: Fully coupled "online" chemistry within the WRF model, Atmos. Environ., 39, 6957–6975, 2005.

Guenther, A., Karl, T., Harley, P., Wiedinmyer, C., Palmer, P. I., and Geron, C.: Estimates of global terrestrial isoprene emissions using MEGAN (Model of Emissions of Gases and Aerosols from Nature), Atmos. Chem. Phys., 6, 3181-3210, doi:10.5194/acp-6-3181-2006, 2006.

Ødemark, K., Dalsøren, S. B., Samset, B. H., Berntsen, T. K., Fuglestvedt, J. S., and Myhre, G.: Short-lived climate forcers from current shipping and petroleum activities in the Arctic, Atmos. Chem. Phys., 12, 1979-1993, 10.5194/acp-12-1979-2012, 2012.

Pfister, G. G., Avise, J., Wiedinmyer, C., Edwards, D. P., Emmons, L. K., Diskin, G. D., Podolske, J., and Wisthaler, A.: CO source contribution analysis for California during ARCTAS-CARB, Atmos. Chem. Phys. Discuss., 11, 3627-3661, doi:10.5194/acpd-11-3627-2011, 2011.

Sessions, W. R., Fuelberg, H. E., Kahn, R. A., and Winker, D. M.: An investigation of methods for injecting emissions from boreal wildfires using WRF-Chem during ARCTAS, Atmos. Chem. Phys., 11, 5719-5744, doi:10.5194/acp-11-5719-2011, 2011.

Stohl, A., Forster, C., Frank, A., Seibert, P., and Wotawa, G.: Technical note: The Lagrangian particle dispersion model FLEXPART version 6.2, Atmos. Chem. Phys., 5, 2461-2474, doi:10.5194/acp-5-2461-2005, 2005.

Thomas, J. L., Raut, J.-C., Law, K. S., Marelle, L., Ancellet, G., Ravetta, F., Fast, J. D., Pfister, G., Emmons, L. K., Diskin, G. S., Weinheimer, A., Roiger, A., and Schlager, H.: Pollution transport from North America to Greenland during summer 2008, Atmos. Chem. Phys., 13, 3825-3848, doi:10.5194/acp-13-3825-2013, 2013.

Wiedinmyer, C., Quayle, B., Geron, C., Belote, A., McKenzie, D., Zhang, X., O'Neill, S., Klos, K., and Wynne, K. K.: Estimating emissions from fires in North America for air quality modelling, Atmos. Environ., 40, 3419–3432, 2006.

Wiedinmyer, C., Akagi, S. K., Yokelson, R. J., Emmons, L. K., Al-Saadi, J. A., Orlando, J. J., and Soja, A. J.: The Fire INventory from NCAR (FINN): a high resolution global model to estimate the emissions from open burning, Geosci. Model Dev., 4, 625-641, doi:10.5194/gmd-4-625-2011, 2011.